LA-7726-MS

Informal Report

Ventilation System Pressure Transients

Small-Scale Shock Tube Results

LOS ALAMOS SCIENTIFIC LABORATORY
Post Office Box 1663 Los Alamos, New Mexico 87545

This work was supported by the US Department of Energy, Division of Waste Management, Production, and Reprocessing.

LA-7726-MS
Informal Report
UC-38
Issued: April 1979

Ventilation System Pressure Transients

Small-Scale Shock Tube Results

D. LaPlante*
P. R. Smith**
W. S. Gregory

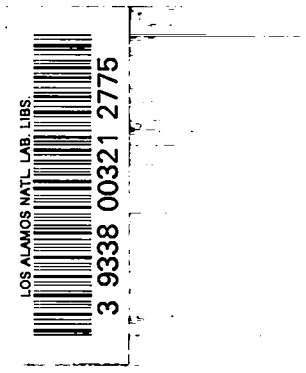

*New Mexico State University, Department of Mechanical Engineering, P.O. Box 3450, University Park, NM 88003.
**Consultant. New Mexico State University, Department of Mechanical Engineering, P.O. Box 3450, University Park, NM 88003.

VENTILATION SYSTEM PRESSURE TRANSIENTS

Small-Scale Shock Tube Results

by

D. LaPlante, P. R. Smith, W. S. Gregory

ABSTRACT

A shock tube is proposed as a means of generating pressure pulses that simulate explosion pressures across ventilation system components. This report describes experimental results using a 76-mm-diam shock tube to evaluate a proposed conceptual design for a 914-mm-diam shock tube. Shock tube driver length variation was shown to be an effective method for controlling pressure pulse duration. A double-diaphragm technique proved to be an excellent way to control driver firing pressure using inexpensive diaphragms. We observed no reflected waves from a small high efficiency particulate air filter mounted on the end of the 76-mm-diam shock tube.

I. INTRODUCTION

A shock tube has been proposed as a means of generating pressure pulses to simulate explosion pressures across ventilation system components.[1] The pressure-pulse characteristics obtained in a small shock tube are described in this report. The small shock tube was operated in a manner similar to that proposed for full-scale testing of high efficiency particulate air (HEPA) filters in a larger shock tube. Pulse amplitudes and durations were predicted on the basis of theoretical relations for the gas dynamics within the shock tube. The pulse amplitudes and durations were then measured and compared with the theoretical predictions. Three shock tube driver section lengths were used to demonstrate the effectiveness of this variable in controlling pulse duration and to ascertain the difference between actual and predicted pulse duration.

II. TEST FACILITY DESCRIPTION

An existing 76-mm-diam shock tube was modified for this study. Figures 1 and 2 show the pertinent details of the shock tube and instrumentation. The major portion of data was obtained using a single 0.05-mm Mylar diaphragm scored to rupture at a driver pressure between 413.7 kPa and 620.5 kPa. Air was used for both the driver and driven gas. The driven section of the shock tube was at atmospheric pressure at the instant of diaphragm rupture for all firings.

Several firings were made using two Mylar diaphragms separated by 229 mm. The total pressure drop across the double-diaphragm section is made large enough to break a single diaphragm, but the shock tube does not fire until the hold-off pressure between the diaphragms is reduced (this method of controlling the firing pressure was suggested in Ref. 3).

Pulse amplitude at three locations on the shock tube was measured for each test run (Fig. 2). However, two of the pulse amplitude measurements (PG_1 and PG_2) were only used to ensure that the shock tube was operating properly. The third pulse amplitude and its duration were measured at the pulse observation point shown in Fig. 2. Distance D_2 was varied from 30 diameters (2.28 m) to 55 diameters (4.18 m) downstream from the diaphragm.

III. TEST RESULTS

A. Pulse Duration Selection by Variation of Driver Length.

Table I summarizes some of the test results, and Figs. 3-5 are photographs of oscilloscope traces representing the pressure pulses obtained. Both measured and theoretical results are given in Table I. Each test run was repeated to ensure reproducibility, which was good except for runs 13 and 14. In these runs, the driver section (D_1) was short so that the expansion wave could catch up with the shock wave before the shock wave arrived at the pulse observation point. The relations used to arrive at the theoretical values are presented in the Appendix. Except for the pulse durations obtained with the shortest driver section, there is good agreement between measured and predicted values. For any given driver length (D_1), a decrease in pulse amplitude (P_2) is evident from the data as the point of observation moves down the tube from 30 to 55 diameters. This is an expected characteristic; however, an estimate of

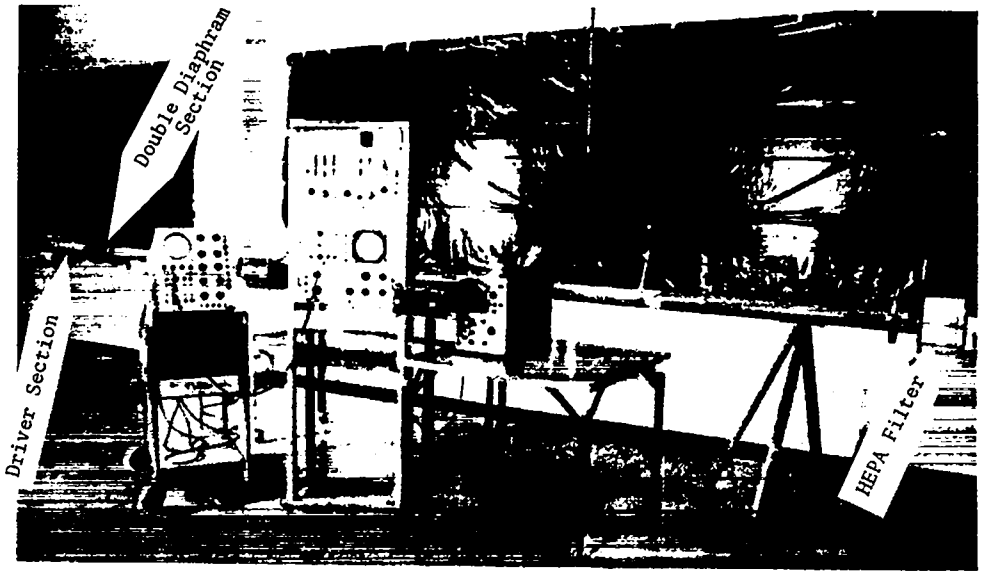

Fig. 1.
Shock tube and instrumentation.

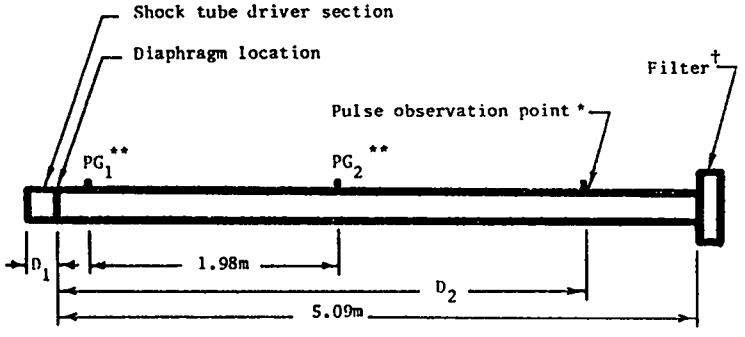

D_1 (driver section lengths): 0.25m, 0.91m, 1.83m

D_2 (pulse observation points): 2.28m, 4.18m, 4.88m

*Pressure pulse data were obtained using a National Semiconductor pressure transducer (LX1720 G) and a Tektronix 564 storage oscilloscope.

**Fast response pressure transducers (Kistler Piezotrons) were used to start and stop a Beckman timer for verification that shock tube was operating properly.

†A HEPA filter was mounted at the end of the shock tube for selected firings. In all other cases the end of the shock tube was open to the atmosphere.

Fig. 2.
Schematic of shock tube showing location of instrumentation and relationship of parameters D_1 and D_2.

TABLE I

MEASURED AND THEORETICAL VALUES FOR
SELECTED DISTANCES AND PULSE AMPLITUDES

Test Run Number	D_1[a] (m)	D_2[b] (m)	Pulse Duration[c] (ms)		Pulse Amplitude (kPa)	
			Theory	Measured	Theory	Measured[d]
1	1.83	2.28	8.6	9.0	124.0	179.3
2	1.83	2.28	8.7	9.5	110.3	158.6
3	1.83	4.18	8.3	9.0	124.0	110.3
4	1.83	4.18	8.3	8.5	124.0	124.0
5	0.91	2.28	4.1	4.5	117.2	131.0
6	0.91	2.28	4.1	4.5	124.0	144.8
7	0.91	2.28	4.1	4.5	124.0	151.7
8	0.91	4.18	3.4	4.0	117.2	89.6
9	0.91	4.18	3.4	4.0	117.2	110.3
10	0.23	2.28	0.4	1.3	124.0	117.2
11	0.23	2.28	0.4	1.2	117.2	117.2
12	0.23	2.28	0.4	1.2	131.0	124.0
13	0.23	4.18	- 0.27	0.7	131.0	75.8
14	0.23	4.18	- 0.26	0.6	144.8	103.4

---

a
Driver section length, m.

b
Distance from diaphragm to pressure measurement location (m). Distance 2.28 m corresponds to 30 diameters down the shock tube, and 4.18 m corresponds to 55 diameters.

c
Pulse duration has been calculated and measured as the time between arrival of shock wave and as arrival of leading edge of expansion wave.

d
Estimated average; amplitude is not constant across top of pulse.

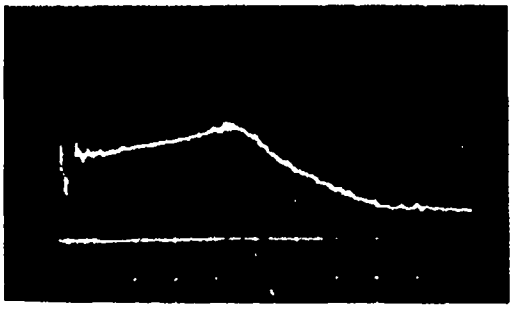

(a)
72.4 kPa/cm vertical, 2 ms/cm horizontal
D_1 = 1.83 m D_2 = 2.28

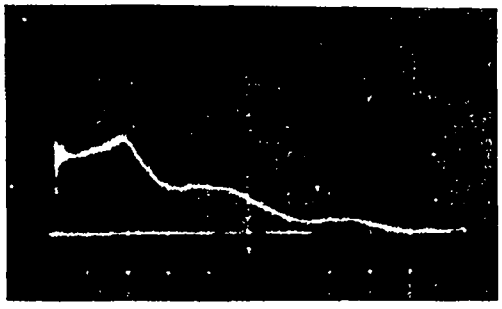

(b)
72.4 kPa/cm vertical, 5 ms/cm horizontal
D_1 = 1.83 D_2 = 2.28 m

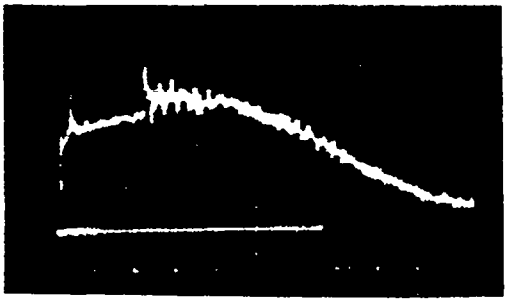

(c)
36.8 kPa/cm vertical, 2 ms/cm horizontal
D_1 = 1.83 D_2 = 4.18 m

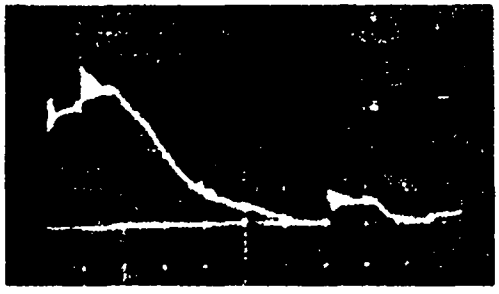

(d)
36.8 kPa/cm vertical, 5 ms/cm horizontal
D_1 = 1.83 m D_2 = 4.18 m

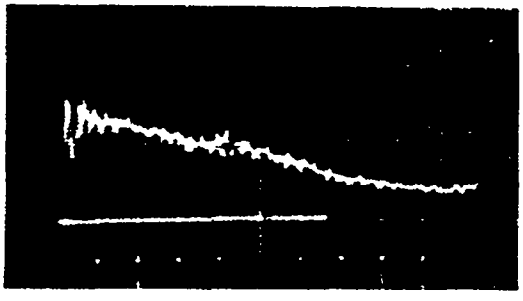

(e)
37.9 kPa/cm vertical, 2 ms/cm horizontal
D_1 = 1.83 m D_2 = 4.88 m

This test run shows the effect of the filter on pressure pulse waveform, and the data are not listed in Table I. Here D_2 is located at 4.18 m plus 9 additional diameters.

Fig. 3.
Comparison of pressure pulse oscilloscope traces for selected test runs.

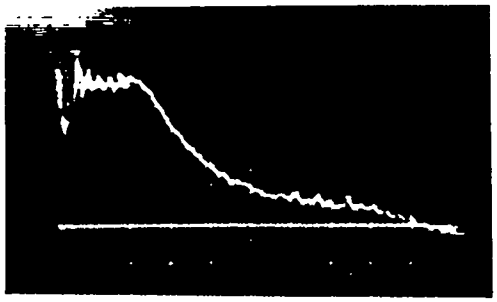

(a)
36.8 kPa/cm vertical, 2 ms/cm horizontal
D_1 = 0.91 m D_2 = 2.28 m

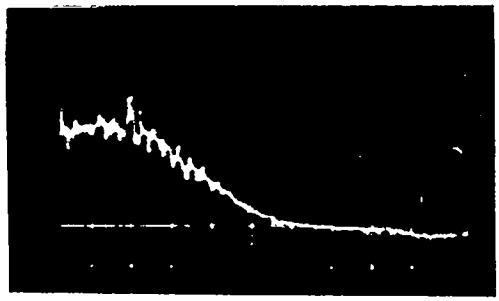

(b)
37.9 kPa/cm vertical, 2 ms/cm horizontal
D_1 = 0.91 m D_2 = 4.18 m

Fig. 4.
Comparison of pressure pulse oscilloscope traces for selected test runs.

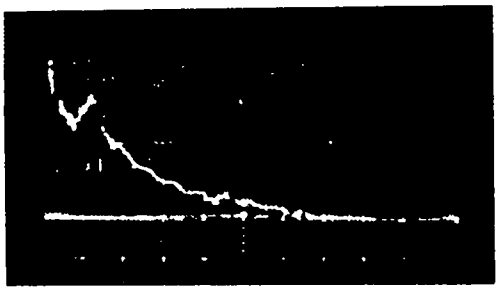

(a)
36.9 kPa/cm vertical, 1 ms/cm horizontal
D_1 = 0.23 D_2 = 2.28 m

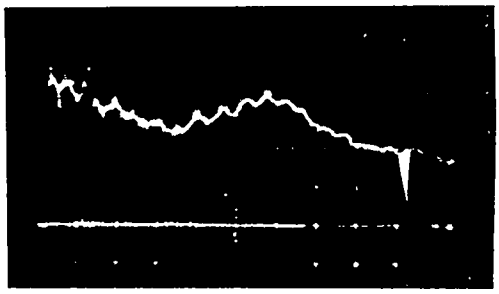

(b)
36.8 kPa/cm vertical, 0.2 ms/cm horizontal
D_1 = 0.23 D_2 = 2.28 m

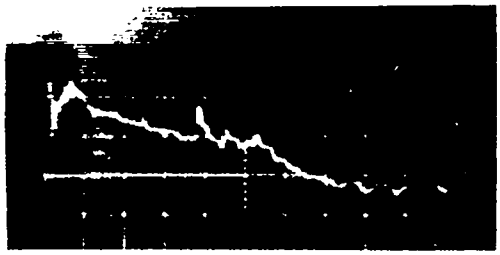

(c)
37.9 kPa/cm vertical, 1 ms/cm horizontal
D_1 = 0.23 m D_2 = 4.18 m

Fig. 5.
Comparison of pressure pulse oscilloscope traces for selected test runs.

attenuation with distance has not been included in the theoretical relations in the Appendix. Decrease in shock amplitude with distance down the tube is greater with smaller shock tube diameters.[2] Therefore, we expect to see less attenuation in the proposed 914-mm-diam tube than is suggested by the data from our 76-mm-diam tube.

Table II gives some pulse decay time constants observed for several combinations of lengths D_1 and D_2. These figures show that pulses tend to have longer decay times as distance down the shock tube increases. Pulse photographs in Figs. 3(a), 3(c), and 3(e) also illustrate this tendency. The data in Table II help explain the pulse obtained when we attempted to produce a 0.4-ms pulse using a driver length of 0.23 m (see Fig. 5(a)). From Table II the pulse decay time constant when D_2 is equal to 2.28 m and D_1 is equal to 0.23 m can be predicted to be approximately 1.8 ms. This is obtained by interpolating the values obtained when D_1 equals 0.91 m and 1.83 m. From Fig. 5(a) the time constant appears to be 1.5 ms if the peak at 1.3 ms is taken as

TABLE II

PULSE DECAY TIME CONSTANTS

D_1 (m)	D_2 (m)	Pulse Decay Time Constant[a] (ms)
1.83	2.28	6.0
1.83	2.28	5.5
1.83	4.18	7.5
1.83	4.18	8.0
0.91	2.28	4.0
0.91	2.28	4.0
0.91	2.28	4.0
0.91	4.18	4.0
0.91	4.18	5.0

[a]Time it takes for a pulse amplitude to decay to 1/e of its initial value.

the beginning of pulse decay. Pressure traces obtained from longer pulse duration measurements agree well with theory and suggest that the peak at 1.3 ms in Fig. 5(a) is the point at which the expansion wave causes decay to begin. A 1.3- or 1.2-ms pulse is significantly longer than the predicted 0.4 ms. For D_1 equal to 0.23 m and D_2 equal to 4.18 m, the theory predicts that the expansion wave will catch up with the shock wave before the shock wave arrives at the observation point. Data in Table I show a consistently longer measured pulse than predicted, the average difference being 0.6 ms. This difference appears to be independent of D_1 and D_2. Adding a constant equal to 0.6 ms to all pulse-duration predictions would bring calculated and measured pulse duration into close agreement. This constant neglected in the theoretical model may be considered a correction for the inertia of the system.

Two things should be noted. A pulse decay time constant of approximately 1.5 ms for pulses of short duration places a lower limit on the realizable effective pulse. Short pulses are destined to have a sawtooth form rather than the more square waveform of longer pulses.

Slightly different vertical scale factors have been given in the collection of pulse photographs. This is the result of a slight nonlinearity in the pressure transducer calibration curve. The scale factor given in any particular photograph is correct for the magnitude of the pulse's higher pressure points.

B. Effect of Filter on Pressure Pulse Waveform

Several firings were made with a HEPA filter attached to the end of the shock tube. This was done to see what effect, if any, the filter would have on the pressure-pulse waveform. The pulse shown in Fig. 3(e) was recorded from a pressure transducer located 230 mm upstream from the filter. This waveform is typical of two others obtained under the same conditions. The differences between pulses shown in Figs. 3(e) and 3(c) are a filter and nine additional diameters of attenuation. To date, we have observed no significant interference between the generated pressure-pulse waves and the waves reflected from the filter.

C. Control of Firing Pressure with Double Diaphragm

Even the most carefully machine-scored diaphragms will rupture over a narrow range of pressures rather than exactly at their nominal burst pressure. Such carefully made diaphragms are rather expensive for small shock tubes and

would no doubt be very expensive for a 914-mm-diam shock tube. The double-diaphragm approach proposed in Ref. 1 was tried with the 76-mm-diam shock tube and was an excellent way to control the driver pressure with simple diaphragm materials. No difficulty was experienced in pressurizing the driver section to a selected value and then firing the shock tube by venting the intermediate pressure hold-off section to the atmosphere.

Table III presents data obtained from double-diaphragm firings. Comparing Table III with Tables I and II for single-diaphragm firings, we see the following.

1. Pulse durations are essentially the same 30 diameters down the shock tube for both single- and double-diaphragm firings.
2. With the double diaphragm, longer pulse durations were measured at 55 diameters rather than at 30 diameters. This is both contrary to what is expected and to what was found with a single diaphragm. These differences are not large enough to be of concern but are mentioned to show predictive limitations of the theory.
3. The time constant for pulse decay is slightly longer using a double diaphragm.

The pressure amplitudes shown in Table III are higher than those in Table I, partly because the shock tube was fired at higher driver pressures during the double-diaphragm testing. Also, double diaphragms tend to cause higher pressures behind the shock front than do single-diaphragm firings.[3] The 229-mm hold-off section represents three shock tube diameters. As this length is reduced, the observed pulse duration differences between single- and double-diaphragm firings should disappear.

IV. PREDICTED PULSE DURATIONS FOR 914-mm SHOCK TUBE

Calculated pulse durations are in agreement with measured values taken from the 76-mm shock tube that was operated in a region giving shock waves of Mach 1.45 to 1.60. We anticipate that the proposed 914-mm shock tube would be operated up to a maximum of Mach 1.85. We assume that the theoretical shock tube equations remain valid up through this moderately extended Mach range and will be a useful guide in the design of the 914-mm shock tube. Predicted pulse durations as a function of shock tube section lengths are listed in Table IV. These values are the output of the theoretical equations for a driver pressure

TABLE III

DOUBLE DIAPHRAGM DATA

D_1 (m)	D_2 (m)	Pulse Duration (ms) Theory	Pulse Duration (ms) Measured	Pulse Amplitude (kPa) Theory	Pulse Amplitude (kPa) Measured	Pulse Decay Time Constant (ms)
0.91	2.28	4.1	4.5	144.8	179.3	5.5
0.91	2.28	4.1	4.0	151.7	186.2	6.5
0.91	2.28	4.1	4.2	151.7	179.3	5.4
0.91	4.18	3.5	5.0	137.9	110.3	6.5
0.91	4.18	3.5	4.8	151.7	110.3	5.4
0.91	4.18	3.5	5.0	151.7	110.3	6.2
0.91	4.18	3.5	5.0	144.8	103.4	5.8

TABLE IV

PREDICTED PULSE DURATION/DRIVER LENGTH VALUES

D_1 (m)	Pulse Duration (ms) D_2= 27.4 m (30 dia)	Pulse Duration (ms) D_2= 38.1 m (41 dia)
1.52	-0.3[b]	-3.8[b]
3.05	8.4	4.9
4.57	17.1	13.6
6.10	25.8	22.3
7.62	33.6[a]	31.0
9.14	40.4[a]	39.7
10.67	47.3[a]	47.1[a]
12.19	54.1[a]	53.9[a]

---

[a] Contact discontinuity has arrived before expansion wave.

[b] Negative pulse duration prediction is a case of expansion wave having caught up with the shock wave before its arrival at observation point.

of 1724 kPa, a driven section open to local atmospheric pressure, and air in both sections at 24°C.

We believe that even longer dwell times are attainable by increasing the volume of the high-pressure driver section. However, a 50-ms pulse duration will allow us to compare our results with previously derived values.[4]

V. SUMMARY

The experimental results show that varying the shock tube driver length is an effective means of changing the pressure pulse duration. The theoretical and measured values were in agreement within the shock wave region that we expect to operate the 914-mm-diam shock tube. Predicted pulse dwell times of 50 ms should be attainable for the 914-mm-diam shock tube with a 12.2-m driver section and a 38.1-m driven section.

Experimentation with a small HEPA filter at the open end of the 76-mm-diam shock tube was performed. No indication of interference was observed with the generated pressure pulse by reflected waves from the filter.

The double-diaphragm technique proved to be an effective method of controlling driver firing pressure. This method of control should allow us to reduce the diaphragm cost by eliminating the need for machine-scored diaphragms.

APPENDIX

RELATIONS USED TO ESTIMATE DURATION AND AMPLITUDE OF SHOCK TUBE PRESSURE PULSES

Figure A-1(a) shows the regions in the shock tube at time equal zero. Figure A-1(b) shows the regions in the shock tube after bursting the diaphragm but before the expansion wave reaches the driver end of the tube. Symbols describing parameters in each of the shock tube regions and used in deriving relations to estimate duration and amplitude of the shock tube pressure pulses are listed below.

P_i = pressure in region i, kPa

T_i = temperature in region i, °K

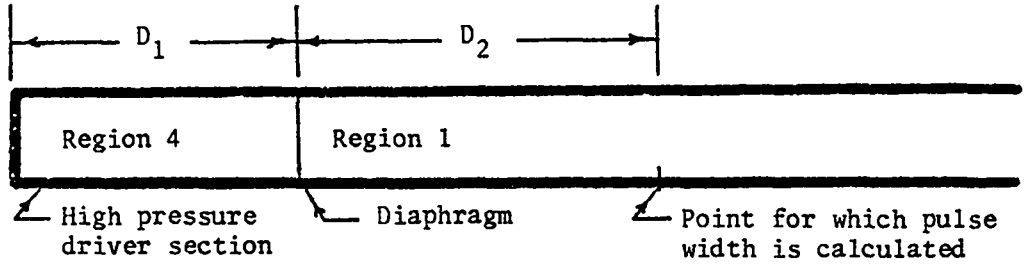

(a)

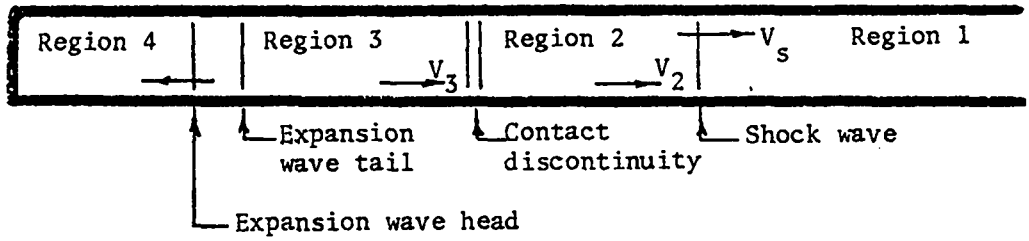

(b)

Fig. A-1.
Shock tube regions before and after bursting diaphragm.

V_i = velocity of gas in region i, m/s

M_s = shock wave Mach number

C_i = speed of sound in region i, m/s

K = specific gas heat ratio

R = universal gas constant for air

V_s = velocity of shock wave

P_4, P_1, T_1, and T_4 are the measured shock tube variables. An open ended shock tube is used so P_1 is known to be equal to the ambient barometric pressure. T_1 and T_4 are assumed equal to the ambient temperature.

$$C_3 = \frac{V_3}{M_3} \tag{A-1}$$

$$V_s = M_s C_1 \tag{A-2}$$

The head of the expansion wave travels through region 4 toward the driver end of the shock tube at the speed of sound (C_4). The tail of the expansion wave, by definition, occurs where the transition from region 4 to region 3 is complete. The tail travels in a gas at temperature T_3 and thus at a speed C_3. Figure A-2 shows the transition between regions 4 and 3 at the instant the expansion wave head reaches end of the driver section.

The transition zone width is $10\ D_1\left(1 - \frac{C_3}{C_4}\right)$. At the instant the expansion wave head reflects, it has velocity C_4; after passing through the transition region it has a velocity of $C_3 + V_3$ toward the open end of the tube. The pulse duration calculation is based on the expansion wave head proceeding at an average velocity of $(C_4 + C_3 + V_3)/2$ through a distance of $1/2\ D_1\left(1 - \frac{C_3}{M_3}\right)$ upon reflection at the driver end. Using a distance of half the transition zone width allows for the fact that the tail is moving toward the reflected head, thereby reducing the transition region distance through which the head must pass.

$$\frac{P_2}{P_1} = \frac{K - 1}{K + 1}\left(\frac{2K}{K - 1} M_s^2 - 1\right) . \tag{A-3}$$

$$\frac{P_4}{P_1} = \frac{P_2}{P_1}\left[1 - \frac{K - 1}{K + 1}\left(\frac{M_s^2 - 1}{M_s}\right)\right]^{\frac{-2K}{K - 1}} . \tag{A-4}$$

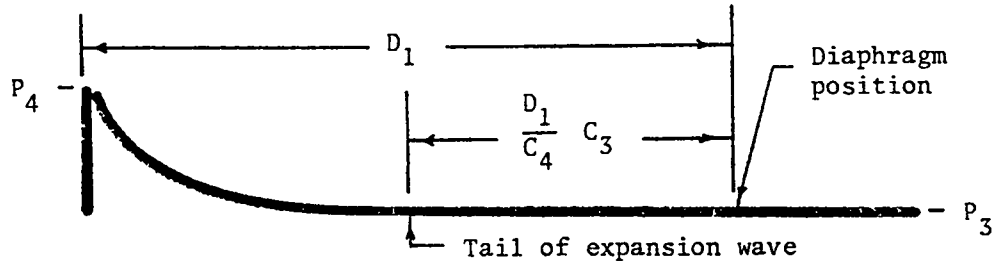

Fig. A-2.
Transition between regions 4 and 3.

Equations (A-3) and (A-4) are used to obtain a value for M_s that yields the ratio of P_4/P_1.

The pulse pressure amplitude P_2 is then available from the known value of P_1.[5]

$$\frac{P_4}{P_3} = \frac{P_4/P_1}{P_2/P_1} \quad \text{because } P_3 = P_2 \ . \tag{A-5}$$

$$\frac{T_2}{T_1} = \frac{2(K-1)\left(1 + \frac{K-1}{2} M_s^2\right)\left(\frac{2K}{K-1} M_s^2 - 1\right)}{M_s^2 \ (K+1)^2} \ , \tag{A-6}$$

from which T_2 is obtained by using known value of T_1.

$$C_1 = KT_1R = C_4, \tag{A-7}$$

$$C_2 = KT_2R. \tag{A-8}$$

$$M_2 = \frac{C_1}{C_2} M_s - \sqrt{\frac{1 + 0.2M_s^2}{1.4M_s^2 - 0.2}} \quad \text{and} \tag{A-9}$$

$$V_2 = M_2C_2 \ . \tag{A-10}$$

$$V_3 = V_2 \ . \tag{A-11}$$

$$M_3 = \frac{\left(\frac{P_4}{P_3}\right)^{\frac{K-1}{2K}} - 1}{(K-1)/2} \tag{A-12}$$

The (t_c) time required for the head of the expansion wave to catch up with the contact discontinuity is

$$t_c = \frac{D_1}{C_4} + \frac{tZ/2}{\left(C_4 + C_3 + V_3\right)^2} + \frac{D_1 - tZ/2}{C_3 + V_3} + \frac{V_2 t_c}{C_3 + V_3}$$

$$= \left(\frac{D_1}{C_4} + \frac{tZ}{C_4 + C_3 + V_3} + \frac{D_1 - tZ/2}{C_3 + V_3} \right) \Bigg/ \left(1 - \frac{V_2}{C_3 + V_3} \right) \qquad \text{(A-13)}$$

where $tZ = D_1\left(1 - \frac{C_3}{C_4}\right)$. Let t_E be the time required for the head of the expansion wave to arrive at the observation point (a distance D_2 downstream from the diaphragm). t_E will depend on whether the contact surface has preceded the expansion head at the observation point. If the expansion head travels through region 2 before arriving at the observation point, it will be for a distance

$$X_2 = D_2 - T_c V_2 \quad . \qquad \text{(A-14)}$$

Then

$$t_E = \frac{D_1}{C_4} + \frac{tZ}{C_4 + C_3 + V_3} + \frac{D_1 - tZ/2 + D_2}{C_3 + V_3} \text{ when } X_2 \leq 0 \text{ and} \qquad \text{(A-15)}$$

$$t_E = \frac{D_1}{C_4} + \frac{tZ}{C_4 + C_3 + V_3} + \frac{D_1 - tZ/2 + t_c V_2}{C_3 + V_3} + \frac{X_2}{C_2 + V_2} \text{ when } X_2 > 0 \quad . \qquad \text{(A-16)}$$

The time (t_s) between diaphragm rupture and arrival of the shock wave at the observation point is

$$t_s = \frac{D_2}{M_s C_1} \quad . \qquad \text{(A-17)}$$

Pulse duration is calculated as the time interval between arrival of the shock wave and arrival of the expansion wave head at the observation point.

$$\text{Pulse duration} = t_E - t_s \qquad \text{(A-18)}$$

REFERENCES

1. W. S. Gregory and P. R. Smith, "Ventilation System Pressure Transients - Shock Tube Conceptual Design," Los Alamos Scientific Laboratory report LA-7413-MS (September 1978).

2. R. J. Emrich and C. W. Curtiss, "Attenuation in the Shock Tube," Appl. Phys. 24, 360 (1953).

3. R. H. Bacue, "The Double Diaphragm Shock Tube," MSME Thesis, New Mexico State University (1973).

4. W. L. Anderson and T. Anderson, "Effects of Shock Overpressure on High Efficiency Filter Units," 9th A.E.C. Air Cleaning Conference, September 1966, CONF-660904, Vol. 1.

5. A. J. Chapman and W. F. Walker, Introductory Gas Dynamics (Holt, Rinhart and Winston, New York, New York, 1971).

Printed in the United States of America. Available from
National Technical Information Service
US Department of Commerce
5285 Port Royal Road
Springfield, VA 22161

Microfiche $3.00

001-025	4.00	126-150	7.25	251-275	10.75	376-400	13.00	501-525	15.25
026-050	4.50	151-175	8.00	276-300	11.00	401-425	13.25	526-550	15.50
051-075	5.25	176-200	9.00	301-325	11.75	426-450	14.00	551-575	16.25
076-100	6.00	201-225	9.25	326-350	12.00	451-475	14.50	576-600	16.50
101-125	6.50	226-250	9.50	351-375	12.50	476-500	15.00	601-up	

Note: Add $2.50 for each additional 100-page increment from 601 pages up.